

DOI: <https://doi.org/10.17816/PTORS568295>

Original Study Article



Comparative evaluation of contusion spinal cord injury models from ventral and dorsal approaches in rabbits in an experiment

Anton S. Shabunin^{1,2}, Margarita V. Savina¹, Timofey S. Rybinskikh¹, Anna D. Dreval¹, Vladislav D. Safarov^{1,2}, Platon A. Safonov¹, Andrey M. Fedyuk¹, Daria A. Sitovskaia³, Nikita M. Dyachuk¹, Alexandra S. Baidikova¹, Lidia S. Konkova¹, Olga L. Vlasova², Sergei V. Vissarionov¹

¹ H. Turner National Medical Research Center for Children's Orthopedics and Trauma Surgery, Saint Petersburg, Russia;

² Peter the Great Saint Petersburg Polytechnic University, Saint Petersburg, Russia;

³ Polenov Neurosurgical Institute, Saint Petersburg, Russia

ABSTRACT

BACKGROUND: Contemporary experimental models for spinal cord injury studies are mainly based on spinal cord injury in rats and mice. Modeling of experimental spinal cord injuries is generally performed from the dorsal approach, which excludes its injury as a result of compression by the fragments of the fractured vertebral body and significantly restricts the application of the results obtained from clinical practice.

AIM: To develop and create contusional spinal cord injury model from the ventral approach with its subsequent comparison with the contusional spinal cord injury model from the dorsal approach.

MATERIALS AND METHODS: The study examined 20 female Soviet Chinchilla rabbits weighing 3.5–4.5 kg. The rabbits were subjected to standardized spinal cord injuries from the ventral and dorsal approaches at the L_{II} level. Somatosensory- and motor-evoked potentials, H-reflex, were recorded in all experimental animals before injury, immediately after, and 3 and 8 h after injury. Histological studies were also performed using qualitative and semiquantitative analyses of biopsy samples of damaged areas and assessing the number of dystrophic neurons over time. The results of neurophysiological and histological examinations of the spinal cord in cases of ventral and dorsal trauma were statistically processed.

RESULTS: When modeling spinal cord injury from the ventral approach, in comparison with the model from the dorsal approach, more significant damage is detected. As a result of the injury factor, the dysfunction of both neurons at the traumatization level and peripheral neurons below the injury zone was revealed; however, as histological examinations have shown, in contrast to the dorsal approach, mild hemorrhage was observed in the ventral approach.

CONCLUSIONS: The results obtained indicate a more significant and strict contusion mechanism of the spinal cord injury model from the ventral approach and the maximum proximity of the resulting model in a clinical situation. In the future, the experimental model of the contusional spinal cord injury in a laboratory animal can be used in chronic experiments.

Keywords: spinal cord injury; contusion spinal cord injury; rabbit; model.

To cite this article

Shabunin AS, Savina MV, Rybinskikh TS, Dreval AD, Safarov VD, Safonov PA, Fedyuk AM, Sitovskaia DA, Dyachuk NM, Baidikova AS, Konkova LS, Vlasova OL, Vissarionov SV. Comparative evaluation of contusion spinal cord injury models from ventral and dorsal approaches in rabbits in an experiment. *Pediatric Traumatology, Orthopaedics and Reconstructive Surgery*. 2023;11(4):487–500. DOI: <https://doi.org/10.17816/PTORS568295>

Received: 12.08.2023

Accepted: 25.10.2023

Published: 20.12.2023

УДК 616.832-001-089-092

DOI: <https://doi.org/10.17816/PTORS568295>

Оригинальное исследование

Сравнительная оценка моделей контузионной травмы спинного мозга из вентрального и дорсального доступов у кроликов в эксперименте

А.С. Шабунин^{1, 2}, М.В. Савина¹, Т.С. Рыбинских¹, А.Д. Древаль¹, В.Д. Сафаров^{1, 2},
П.А. Сафонов¹, А.М. Федюк¹, Д.А. Ситовская³, Н.М. Дячук¹, А.С. Байдикова¹, Л.С. Конькова¹,
О.Л. Власова², С.В. Виссарионов¹

¹ Национальный медицинский исследовательский центр детской травматологии и ортопедии имени Г.И. Турнера, Санкт-Петербург, Россия;

² Санкт-Петербургский политехнический университет Петра Великого, Санкт-Петербург, Россия;

³ Российский научно-исследовательский нейрохирургический институт имени профессора А.Л. Поленова, Санкт-Петербург, Россия

АННОТАЦИЯ

Обоснование. Современные экспериментальные модели для изучения позвоночно-спинномозговой травмы преимущественно основаны на повреждении спинного мозга у крыс или мышей. Как правило, моделирование экспериментальных травм спинного мозга выполняют из дорсального доступа, что исключает его повреждение в результате сдавления отломками тела сломанного позвонка и существенно ограничивает применение полученных результатов с точки зрения клинической практики.

Цель — провести сравнительный анализ экспериментальной модели позвоночно-спинномозговой травмы у кроликов из вентрального доступа с моделью позвоночно-спинномозговой травмы из дорсального доступа.

Материалы и методы. Исследование проводили на 20 самках кроликов породы Советская шиншилла массой 3,5–4,5 кг. Кролики были разделены на две группы и подвергались стандартизированным повреждениям спинного мозга из вентрального и дорсального доступов на уровне позвонка L_{II} (по 10 кроликов в каждой группе). У всех экспериментальных животных регистрировали соматосенсорные, моторные вызванные потенциалы и Н-рефлекс до травмы, сразу после и через 3 и 8 ч после травмы. Выполнены также гистологические исследования с проведением качественного и полуколичественного анализа биопсийных образцов поврежденных участков спинного мозга и оценкой числа дистрофичных нейронов в динамике. Результаты нейрофизиологического и гистологического исследования спинного мозга при вентральной и дорсальной травмах подвергли статистической обработке.

Результаты. При моделировании травмы спинного мозга из вентрального доступа наблюдается более выраженное его повреждение по сравнению с моделью из дорсального доступа. Выявлено нарушение функций нейронов как на уровне травматизации, так и ниже зоны повреждения. При вентральном доступе отмечена меньшая степень кровоизлияния, чем при дорсальном, по данным гистологического исследования.

Заключение. Полученные результаты указывают на более выраженный строго контузионный механизм повреждения спинного мозга при экспериментальном моделировании травмы из вентрального доступа и максимальную приближенность полученной модели к клинической ситуации. Созданная экспериментальная модель контузионного повреждения спинного мозга у лабораторного животного в дальнейшем может быть использована в хронических экспериментах.

Ключевые слова: позвоночно-спинномозговая травма; контузионная травма спинного мозга; кролик; модель.

Как цитировать

Шабунин А.С., Савина М.В., Рыбинских Т.С., Древаль А.Д., Сафаров В.Д., Сафонов П.А., Федюк А.М., Ситовская Д.А., Дячук Н.М., Байдикова А.С., Конькова Л.С., Власова О.Л., Виссарионов С.В. Сравнительная оценка моделей контузионной травмы спинного мозга из вентрального и дорсального доступов у кроликов в эксперименте // Ортопедия, травматология и восстановительная хирургия детского возраста. 2023. Т. 11. № 4. С. 487–500. DOI: <https://doi.org/10.17816/PTORS568295>

BACKGROUND

Spinal cord injury (SCI) is a pressing medical and social issue because it often results in permanent disability [1]. Despite the vast scientific literature on this topic, the search for effective treatment methods based on the study of pathogenetic mechanisms of trauma disorders in experimental studies is ongoing. However, the results of experimental studies often cannot be implemented into clinical practice, which is due to the difficulty of reproducing in experiments SCI conditions and other pathological processes close to the real ones in humans and the species-specific peculiarities of the processes of regeneration and restoration of function of nerve tracts in animal models [2]. Therefore, the improvement of experimental models of SCI in laboratory animals remains an urgent problem in experimental traumatology.

The main biomechanical difference between experimental models of SCI and human SCI is the damage to the dorsal structures of the spinal cord and the use of laminectomy to access them during impact simulation. In most clinical cases, the anterior spinal cord structures are damaged because of impact and compression of the fractured vertebral body fragments.

A review of available reports on known experimental models of SCI in laboratory animals revealed inadequate standardization and reproducibility of these animal models, except mice or rats that have an extensive database of publications and relevant criteria for assessing both the severity of experimental traumatic injury and subsequent recovery [3–6]. The use of small rodents for most experiments is related to economic factors such as the relatively low cost of the experiment for long-term studies. However, the use of small rodents as models has some limitations in studying the sequelae of SCI because of several factors, including the size and physiological characteristics of the experimental animal, anatomical structure of the spinal cord roots, rate of axon regeneration, and risks of spontaneous regeneration of damaged areas [7, 8]. The use of small laboratory animals requires an extremely high accuracy of implantation of long-term recording electrodes, which may affect data reproducibility. These reasons explain the rare use of neurophysiological studies in SCI modeling.

According to various authors, the use of standard medium and large animal species for laboratory work is recommended, with rabbits being one of the most promising species for the study of SCI. The peculiarity of the anatomical structure of rabbits is the larger extension of the spinal cord compared with that of rodents. In addition, rabbits have the lowest reparative potential of spinal cord structures among other experimental animals (mice, dogs, cats, guinea pigs, and pigs) [9, 10]. As a laboratory animal, rabbits can serve as optimal models for the assessment of

postoperative status and neurological studies of compression injury and ischemia–reperfusion of the spinal cord because of the peculiarities of its blood supply from the abdominal aorta [11].

Individual scientific papers devoted to the modeling of contusion SCI have reported the results of neurophysiological and histomorphological examinations of the rabbit spinal cord. In these studies, the injury was inflicted from the dorsal side, and the observation was limited to 4 h after SCI from the dorsal approach [12, 13].

To date, the available scientific literature has not presented reproducible models of contusion SCI induced by the ventral approach that would be as close as possible to the clinical situation because of the great complexity of such interventions and the overall labor intensity of experiments for modeling contusion SCI in rabbits.

The aim of this study was to compare a ventral SCI model in rabbits with a dorsal SCI model.

MATERIALS AND METHODS

Research strategy

The study was conducted on 20 female rabbits of the Soviet chinchilla breed weighing 3.5–4.5 kg. The animals were divided into two groups: 10 rabbits subjected to SCI modeling by the ventral approach and another 10 rabbits by the dorsal approach.

Quarantine, maintenance, and preparation of the experimental animals before the operation were performed in accordance with GOST 33216–2014 “Guidelines for Maintenance and Care of Experimental Animals, Rules of Maintenance and Care of Laboratory Rodents and Rabbits.”

All animals were studied electrophysiologically before, immediately after, and 3 and 8 h after SCI application using a Neuro-MVP-8 equipment (Neurosoft, Russia). Motor-evoked potentials (MEPs), somatosensory-evoked potentials (SSEPs), and H-reflex were recorded. The electrodes were placed under combined anesthesia, including the premedication of the animals with xylazine (Rometa, Russia) at a dose of 5 mg/kg, followed by inhalation of 3% sevoflurane vapor. After electrode placement, the animal was anesthetized for 1.5 h to minimize the residual myorelaxant effect of sevoflurane. Baseline neurophysiological parameters were then recorded along with intravenous propofol infusion at a concentration of 4–6 mg/kg/h. After the registration of neurophysiological parameters, SCI was modeled with continued propofol infusion accompanied by nonsteroidal anti-inflammatory drug injections. Neurophysiological parameters were repeatedly recorded immediately and 3 and 8 h after injury. Drugs with myorelaxant effects were not used because of the need to assess motor conduction immediately after injury. The electrocardiogram and respiratory rate of the animals were monitored throughout

the experiment. Animals were sacrificed by intravenous injection of 10% lidocaine solution under general anesthesia 8 h after SCI modeling.

Neurophysiological examinations

The stimulating and recording electrodes for neurophysiological testing were placed according to the schemes shown in Figure 1. These electrodes were surgically implanted to ensure the reproducibility of the neurophysiological examination results.

Owing to the need for prolonged recording of signals at different time intervals, we used cuff electrodes that we manufactured, which were braided with conductive threads based on stainless steel and coated with medical silicone. Two similar strands with uninsulated ends were fixed to the nerve at a standard distance of 1 cm. The total impedance of the system of a pair (active and reference electrodes) of such electrodes when applied to the target area, measured by the built-in functions of the Neurosoft-M software, ranged from 0.8 to 1.0 kOhm.

To record MEPs and SSEPs, the active and reference electrodes were inserted into the spongiosa of the cranial vault bones on both sides of the sagittal line after drilling through the first cortical layer with a 0.3-mm-diameter bone cutter (Fig. 2).

These implantation sites were chosen based on the localization of motor and sensory cortical zones in this area according to rabbit brain atlases [14]. The electrodes implanted in the skull had a stimulating function when recording MEPs and a recording function when recording SSEPs. The intracranial electrodes were made of gold wire. After implantation, the electrodes were fixed with bone cement.

Stimulating electrodes for SSEPs and H-reflex testing were placed on the sciatic nerve of both hind limbs and secured to the surrounding muscles with separate knotted sutures. To record the H-reflex, paired needle electrodes were placed in the flexor muscles of the hind limbs. To record MEPs from the hindlimb muscles, recording electrodes for the H-reflex were used; to record MEPs from the forelimb, paired needle electrodes were placed in the *triceps brachii*. The active recording electrode was placed at the thickness of the muscle belly, and the reference electrode was placed near the tendon of the muscle.

After placing the electrodes to obtain MEPs, the cerebral cortex was electrically stimulated with 0.2 ms of single electrical pulses and 100 mA of stimulation intensity. To record SSEPs, the sciatic nerve was rhythmically stimulated with an electric current with frequency of 0.5 Hz, stimulus duration of 0.2 ms, and stimulus intensity of 2 mA.

When examining the H-reflex, the pulse intensity was gradually increased from 0.2 to 8.0 mA with a step of 0.2 mA to obtain the maximum amplitude of the H- and M-responses during sciatic nerve stimulation.

SCI modeling

Contusive SCI modeling from the ventral approach was conducted according to the author's method reflected in Patent No. 2768486 "Method of Modeling Traumatic Spinal Cord Injury from Ventral Approach in the Lumbar Spine" (2022) [15]. After shaving and treating the surgical field with an alcohol antiseptic solution, an 8–10 cm linear incision of the skin and subcutaneous adipose tissue was made with a scalpel along the pararectal line of the abdomen. The first muscle layer of the anterior abdominal wall

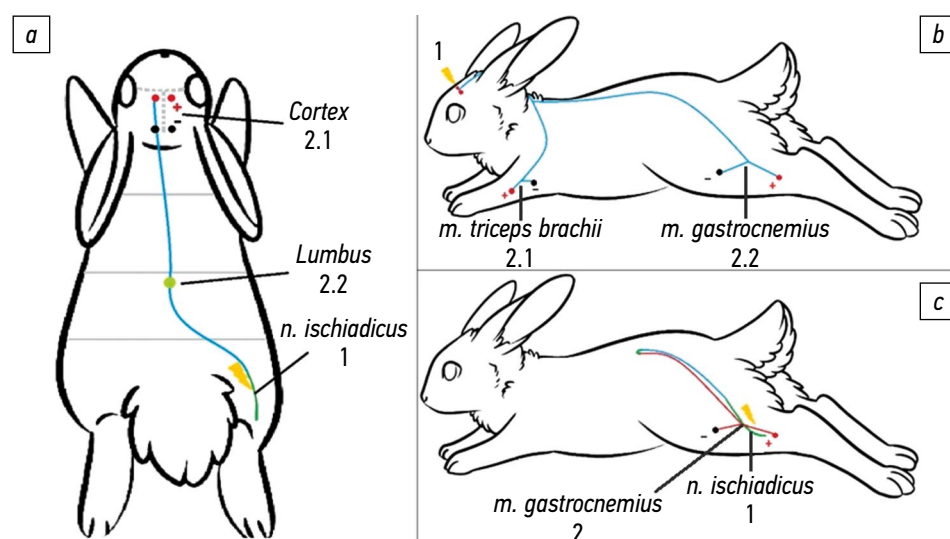


Fig. 1. Scheme of the registration of neurophysiological parameters of the experimental animal: *a*, somatosensory-evoked potentials (1, a stimulating electrode on the sciatic nerve; 2.1, a registering electrode on the cerebral cortex; 2.2, a registering electrode on the lumbar thickness of the spinal cord); *b*, motor-evoked potentials (1, a stimulating electrode in the projection of the motor zone of the cerebral cortex; 2.1, a recording electrode on the triceps brachii; 2.2, a recording electrode on the calf muscle); *c*, H-reflex (1, a stimulating electrode on the sciatic nerve; 2, a recording electrode on the calf muscle)

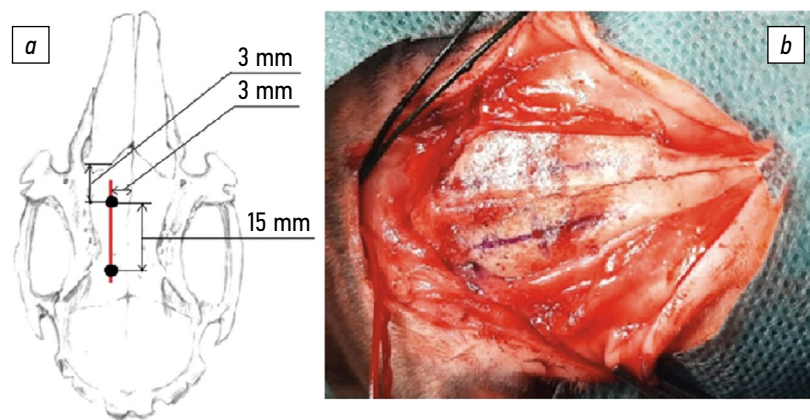


Fig. 2. Scheme of the implantation of intracranial electrodes: *a*, scheme of marking the installation zones of the intracranial electrodes (actively, frontally and referentially, and dorsally), stimulating motor-evoked potentials, and registering somatosensory-evoked potentials; *b*, surgical field with holes prepared for implantation.

(external oblique muscle) was dissected, and the muscle layers up to the spine (external and internal oblique muscles) were dissected using the blunt method. Because of the low thickness and strength of the rabbit peritoneum and the high probability of its damage, the retroperitoneal space was accessed as close to the spine as possible. The internal oblique and transverse muscles were dissected along the edges of the transverse processes. The retroperitoneal space was reexamined, and the L_{II} vertebra was identified. The retroperitoneal tissues and organs were then pushed aside with the scapulae. The L_{II} vertebral body was dissected free of muscle, ligament, and periosteum using a curved Farabeuf dissector and a coagulator. A hole was drilled in the center of the vertebral body using a 3-mm diameter bone mill, and the bone chips were carefully removed. The spinal cord was crushed using a percussion device. The load weighed 100 g, and the free stroke was 30 cm. With this variant of approach to the spinal cord and its damage, the vertebral motor segment in the SCI area did not require stabilization. Hemostasis was then achieved, and the wound was tightly sutured layer by layer.

The impactor consisted of two parts. The impactor was a 20-cm long metal rod and weighing 15 g, with an additional weight of 20 g attached to the upper part. The second part

of the device was a metal frame that was kept in a strictly horizontal position during surgery using a special level, with a guide tube attached to the frame (Fig. 3).

In the second group, the SCI was modeled using the dorsal laminectomy approach at the same level (vertebra L_{II}) and the same impact force. Both groups were immobilized throughout the study to avoid displacement and damage to the electrode system.

Histological examination

Rabbits were euthanized 0, 3, and 8 h after injury, and neurophysiological examination was performed. At appropriate time intervals, the spinal canal was opened by dissection, and the spinal cord was removed from the first lumbar segment (L_I) to the fifth lumbar vertebra (L_V). Each specimen was then placed in 10% buffered formalin for 48 h. At autopsy, transverse and longitudinal sections of the spinal cord were obtained. The area of the greatest macroscopic change (spinal cord tissue hemorrhage) was used as a reference point. A transverse section was cut from this area, and longitudinal sections (0.7 cm long) were cut cranially and caudally at the level of the anterior horns of the spinal cord. Transverse sections were then cut again. The material was dehydrated in graded alcohols and



Fig. 3. Photographs of the impact rig in the assembly

embedded in paraffin in a standard manner. Paraffin blocks were microtomed, and 3- μm thick histological sections were obtained and stained with hematoxylin and eosin. Visualization was performed using AxioStar (CarlZeiss, Germany) and LOMO BLM (Russia) microscopes. Micrographs were taken using the MC-CAM camera built into the LOMO BLM microscope. The hemorrhagic area was estimated using MC-View software (Germany), and the number of neurons was estimated using QuPath software (UK).

Statistical data processing

Statistical data analysis was performed using Wolfram Mathematica 11. The normality of distributions was determined using the Shapiro–Wilk test, and differences between groups were determined using the Mann–Whitney U test.

RESULTS

General observations

No intraoperative complications were observed after 20 surgeries to simulate SCI using ventral and dorsal approaches. All experimental animals underwent electrode implantation for neurophysiological study and the injury modeling phase without the need for additional interventions.

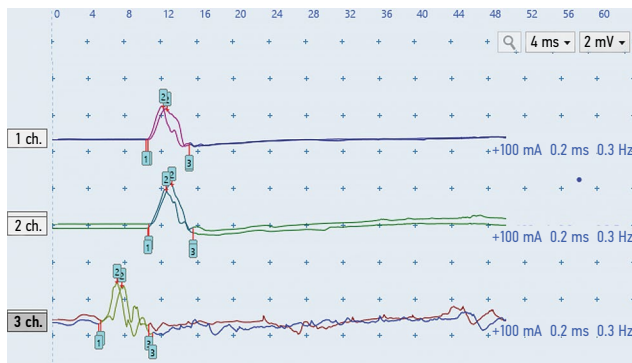


Fig. 4. Motor-evoked potentials from the hind limb (1 and 2 ch.) and forelimb (3 ch.) in a normal rabbit before injury modeling (4 ms/2 mV scale). ch, channel (leads)

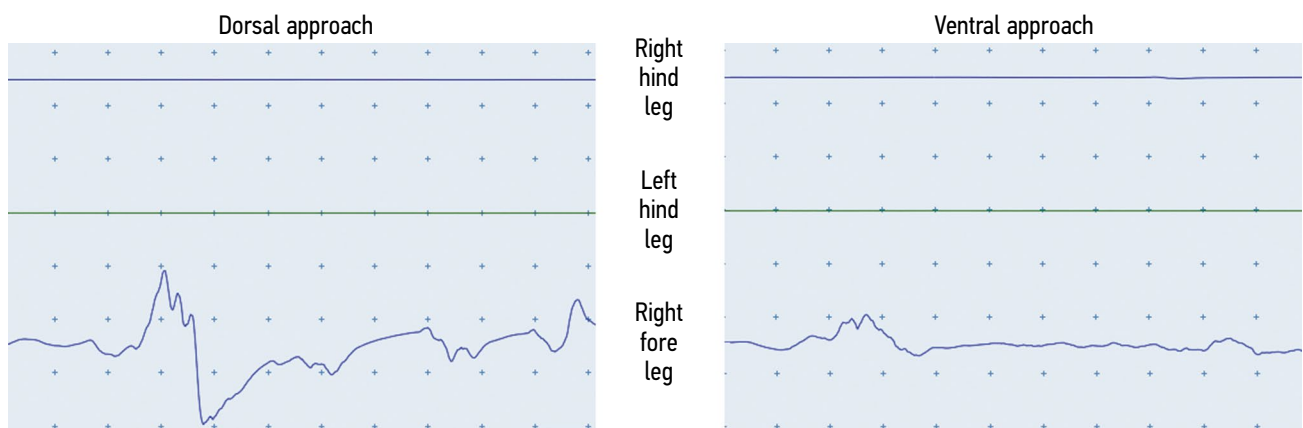


Fig. 5. Motor-evoked potentials 8 h after spinal cord injury modeling from the dorsal and ventral approaches (4 ms/2 mV scale). Motor-evoked potentials from the hind limbs are absent

In the ventral group, high surgical complexity and the need for extremely fast and timely hemostasis after impaction of the impactor were noted. No animal mortality was observed within 8 h after surgery.

Because of the manipulations in both groups, the clinical picture revealed the absence of any motor activity of the hind legs, both voluntary and involuntary, and a lowered tail position, indicating complete damage to the motor pathways of the spinal cord, which was confirmed by neurophysiological examination data.

Results of the neurophysiological examinations

MEPs

In the first and second groups, MEPs were recorded from the muscles of the forelimb and both hind limbs before SCI modeling (Fig. 4). The MEP values in the ventral and dorsal groups were not significantly different ($p > 0.05$), indicating that the animals were comparable between the groups and that the results could be further compared.

Immediately after ventral and dorsal SCI modeling and during the subsequent 8 h, MEPs from the hind limb muscles were not observed, whereas MEPs from the forelimb muscles were preserved, indicating complete disruption of conduction along the motor pathways of the spinal cord at the injury level (Fig. 5).

After SCI simulation with both approaches, the amplitudes of MEPs from the forelimb muscles gradually increased, which significantly increased 8 h after injury ($p = 0.005$) and almost twice the MEP amplitudes before injury (Table).

H-reflex

In the first and second groups, H-reflex and M-response were recorded from the *m. gastrocnemius* before injury modeling, and the indices were comparable in both groups. Comparative analysis of the H-reflex and M-response in the ventral and dorsal groups immediately and 3 and

Table. Indices of motor-evoked potentials recorded from rabbit forelimbs in ventral and dorsal injuries

Group	Index	Before the injury	Immediately after SCI	3 h after SCI	8 h after SCI
DI	Latency, ms	2.67 ± 1.42	4.76 ± 2.42*	4.16 ± 2.21*	4.21 ± 1.11*
	Amplitude, mV	1.63 ± 0.96	1.10 ± 0.47	1.42 ± 0.84	2.81 ± 2.12*
	Duration, ms	9.61 ± 2.36	7.94 ± 1.77	9.28 ± 3.63	8.09 ± 2.18
VI	Latency, ms	2.67 ± 1.42	4.47 ± 2.34*	4.60 ± 2.55*	4.30 ± 0.31*
	Amplitude, mV	1.63 ± 0.96	1.18 ± 0.76	1.98 ± 0.63	2.90 ± 1.82*
	Duration, ms	9.61 ± 2.36	9.50 ± 3.53	8.20 ± 3.05	9.48 ± 3.58

Note. DI, dorsal injury; VI, ventral injury; SCI, spinal cord injury. * Reliability of the difference between the index before and after SCI ($p < 0.05$).

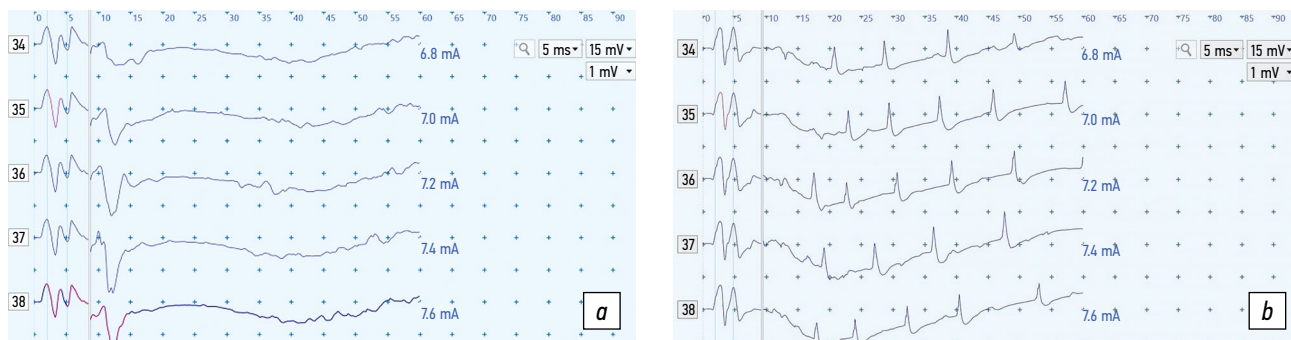


Fig. 6. H-reflex in a rabbit with the dorsal approach before (a) and 8 h after (b) dorsal injury (5 ms/15 mV/1 mV scale): a, H-reflex and M-response are registered before injury; b, polysynaptic responses are registered in large numbers 8 h after injury

8 h after injury were not significantly different between the groups ($p = 0.2$). In 70% of the observations in the ventral and dorsal groups, a significant asymmetry of the H-reflex and M-response was found between the right and left sides ($p = 0.03$), which occurred immediately after injury and increased 3 and 8 h after injury in both groups.

The peculiarities of H-reflex registration in rabbits were found as irregular additional responses in the range of 25–60 ms, visually similar to the H-reflex but differed in the time of appearance, which are described as polysynaptic responses. Such H-reflex changes were observed in 50% of rabbits before injury. After SCI modeling, polysynaptic responses were recorded in the dorsal group in 90% of the observations. The amplitude and frequency of polysynaptic responses gradually increased, reaching their maximum values 8 h after injury (Fig. 6). In 80% of the observations with the dorsal approach, this spontaneous activity acquired a rhythmic character. In contrast, the number and amplitude of polysynaptic responses significantly decreased in the ventral group when compared with that in the dorsal group ($p = 0.001$). Polysynaptic responses after ventral injury were registered in only 10% of the patients.

SSEPs

In the study of SSEPs in rabbits before injury, in response to the stimulation of the sciatic nerve on both sides, an evoked potential from the level of lumbar thickening and a cortical potential from projection areas of the cortex were recorded (Fig. 7).

Latencies and amplitudes of the lumbar thickening and cortical potentials were used to assess SSEPs. In a comparative analysis of SSEP indices before SCI modeling, no significant differences were found between the first and second groups ($p = 0.8$).

The latency of evoked responses is a stable indicator for evaluation, whereas the amplitude of SSEPs in rabbits is variable and depends on the animal characteristics.

Immediately after ventral SCI, cortical SSEPs were absent in all rabbits (Fig. 8). Moreover, 3 and 8 h after injury, cortical responses was not recovered. Immediately after the dorsal SCI modeling, cortical SSEPs were absent in 1 of 10 rabbits (10%) and were reduced in the remaining animals. At 3 h after injury, SSEPs were already absent in 5 of 10 rabbits, and the rest

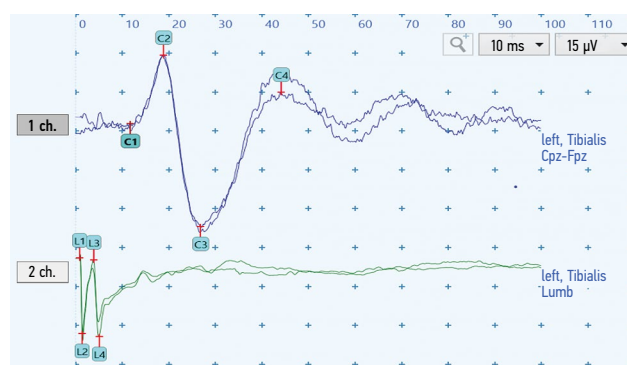


Fig. 7. Somatosensory-evoked potentials in normal rabbits; 1 ch., evoked potential from the projection zones of the cerebral cortex; 2 ch., evoked potential from the level of lumbar thickening (10 ms/15 μ V scale). ch, channel (leads)

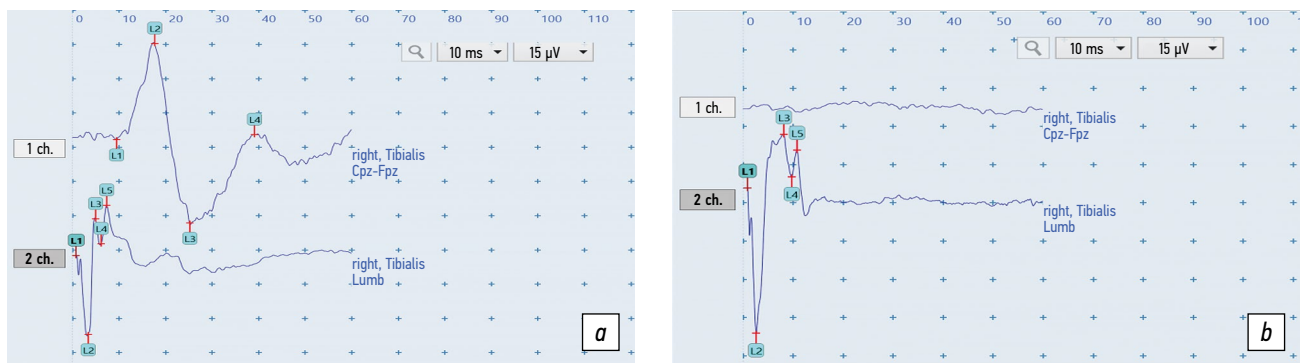


Fig. 8. Somatosensory-evoked potentials in a rabbit before (*a*) and after (*b*) injury: the first channel showed cortical responses, whereas the second channel presented responses from the lumbar level (10 ms/15 μ V scale): *a*, spinal and cortical potentials are registered before injury; *b*, a potential from the lumbar level is registered after injury, and there is no cortical response, indicating a complete disruption of conduction along the somatosensory pathways of the spinal cord at the injury level. The amplitudes of the lumbar response are increased. ch, channel (leads)

showed a progressive decrease in amplitude ($p = 0.005$). At 8 h after dorsal injury, no cortical potentials were recorded.

Thus, after ventral SCI, complete disturbance of spinal cord conduction occurred immediately, whereas after dorsal SCI, it progressed gradually; complete conduction disturbance was observed in all animals 8 h after injury.

Registration of SSEPs 8 h after ventral and dorsal injuries revealed a twofold increase in the amplitude of the potential from the level of lumbar thickening (Fig. 9), and the degree of amplitude increase was significantly predominant in the dorsal group ($p = 0.001$).

Histologic pattern

All spinal cord samples showed multiple hemorrhages in the injury site. SCI specimens from the dorsal group showed more massive and extensive hemorrhages of mostly unchanged erythrocytes, mainly affecting the white matter in the posterior and lateral canaliculi. The hemorrhage area ranged from 10% to 38% of the area of the spinal cord transverse section (Fig. 10*a, b*). In the specimens obtained during SCI modeling in the ventral group, the hemorrhages were small focal hemorrhages involving only the gray matter; the hemorrhage area ranged from 2.3% to 14% of

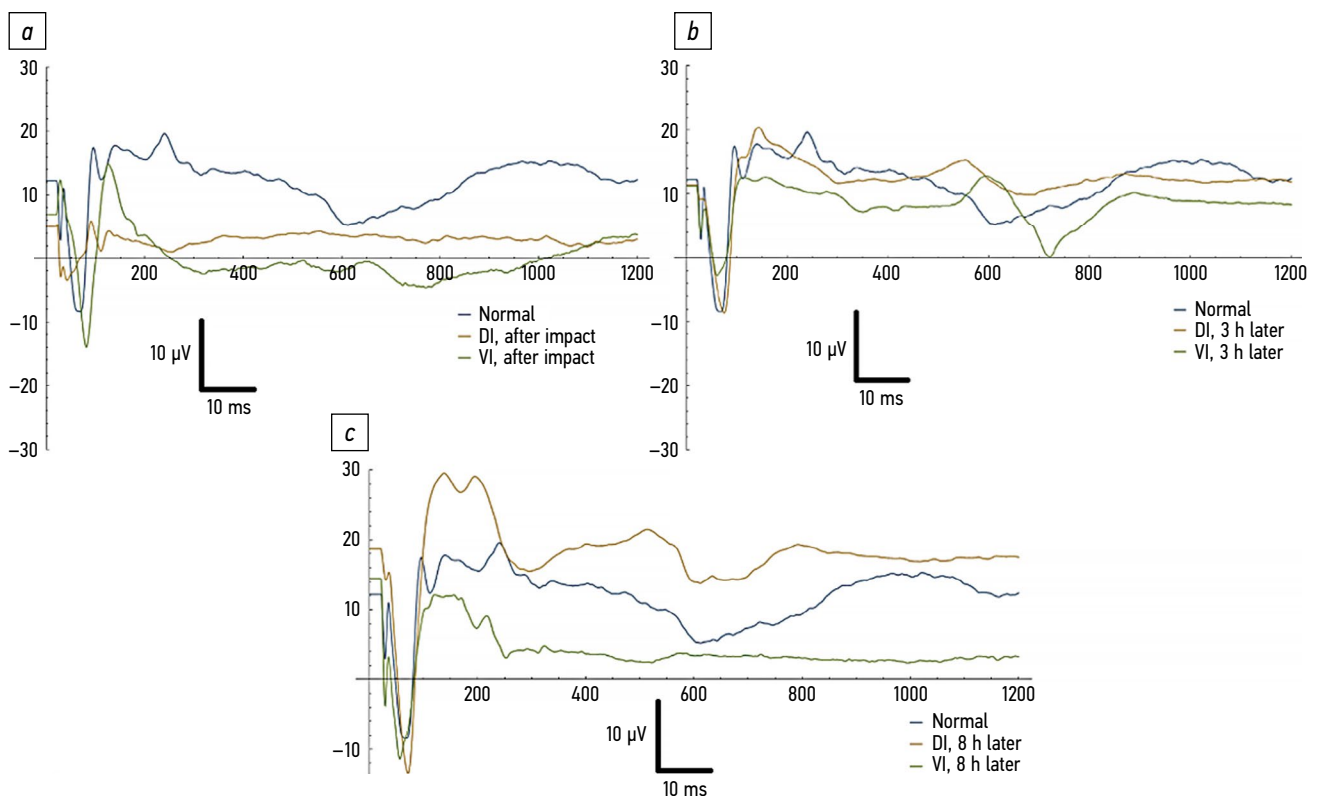


Fig. 9. Comparison of somatosensory-evoked potential curves during withdrawal from lumbar thickening after spinal cord injury modeling using ventral and dorsal approaches: *a*, immediately after injury; *b*, at 3 h; *c*, at 8 h. At 8 h after injury, the amplitude of somatosensory-evoked potentials during withdrawal from the lumbar thickening increased. DI, dorsal injury; VI, ventral injury

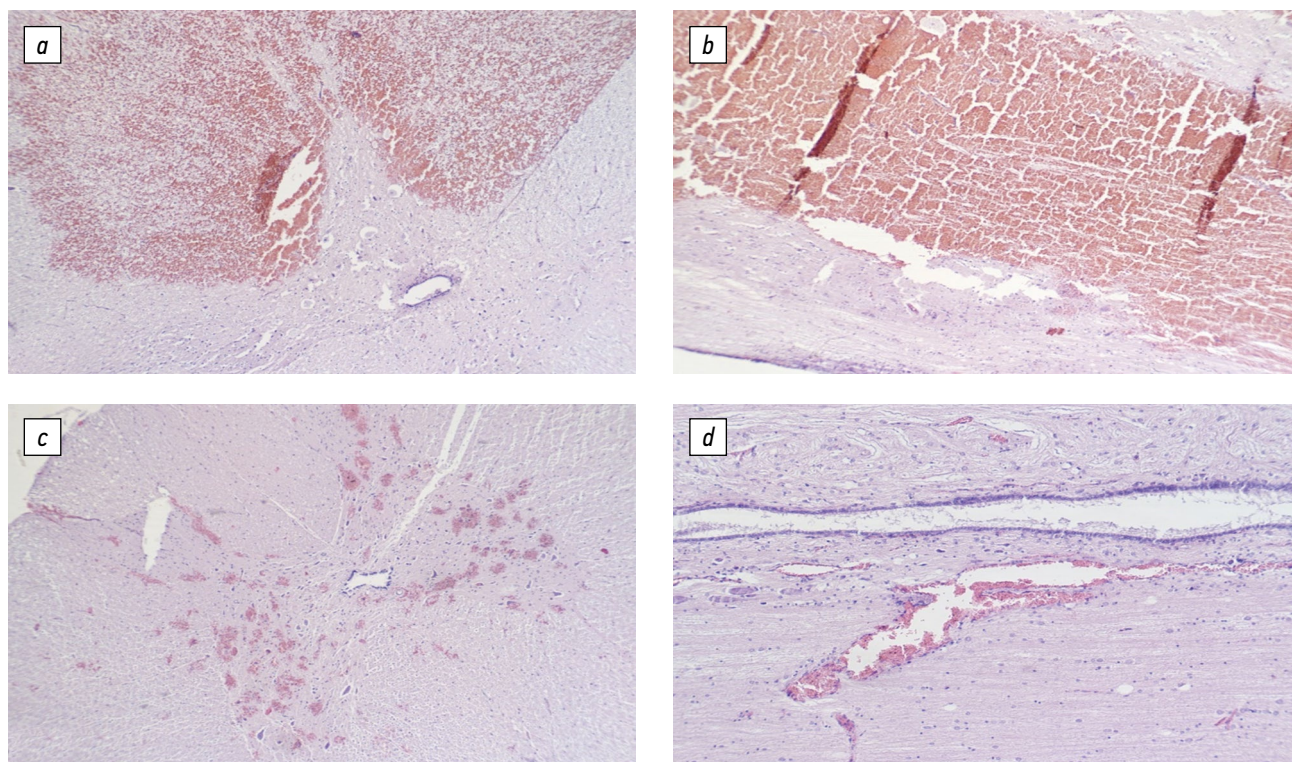


Fig. 10. Hemorrhages in the spinal cord injury area, hematoxylin and eosin staining: *a*, dorsal injury, massive hemorrhage in the area of anterior and lateral tubules (transverse section, $\times 50$); *b*, dorsal injury, massive hemorrhage in the area of anterior and lateral tubules (longitudinal section, $\times 50$); *c*, ventral trauma, small focal hemorrhages in the gray matter of the spinal cord (transverse section, $\times 50$); *d*, ectasized vessel with thrombotic masses in the lumen (longitudinal section, $\times 100$)

the area of the spinal cord transverse section (Fig. 10c). At 8 h after injury, neutrophilic granulocytes accumulated in the hemorrhagic foci: up to 40–50 in one field of view at $\times 400$ magnification. In addition, ectasized vessels

with thrombotic masses in the lumen were visualized in the specimens (Fig. 10d).

All spinal cord specimens showed edema and unfolding of the gray and white matter neuropil 8 h after injury. Changes

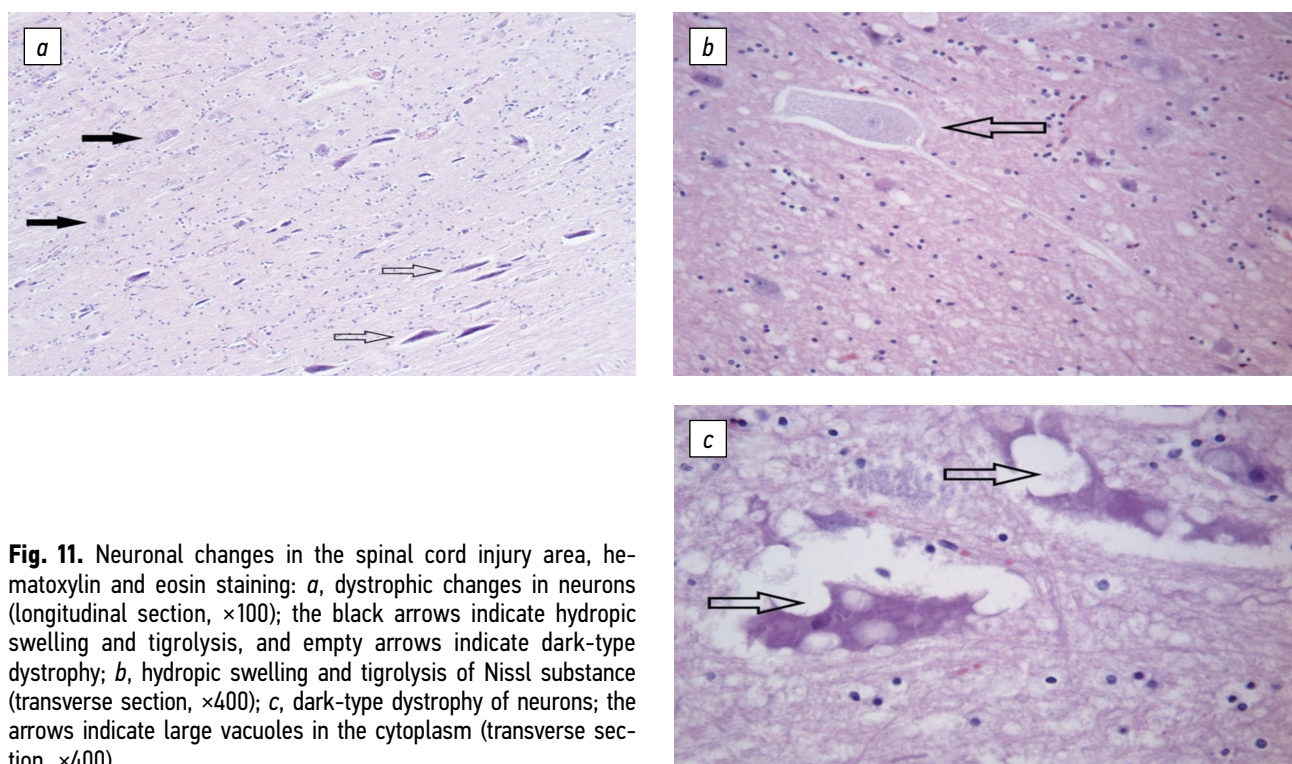


Fig. 11. Neuronal changes in the spinal cord injury area, hematoxylin and eosin staining: *a*, dystrophic changes in neurons (longitudinal section, $\times 100$); the black arrows indicate hydropic swelling and tigrolysis, and empty arrows indicate dark-type dystrophy; *b*, hydropic swelling and tigrolysis of Nissl substance (transverse section, $\times 400$); *c*, dark-type dystrophy of neurons; the arrows indicate large vacuoles in the cytoplasm (transverse section, $\times 400$)

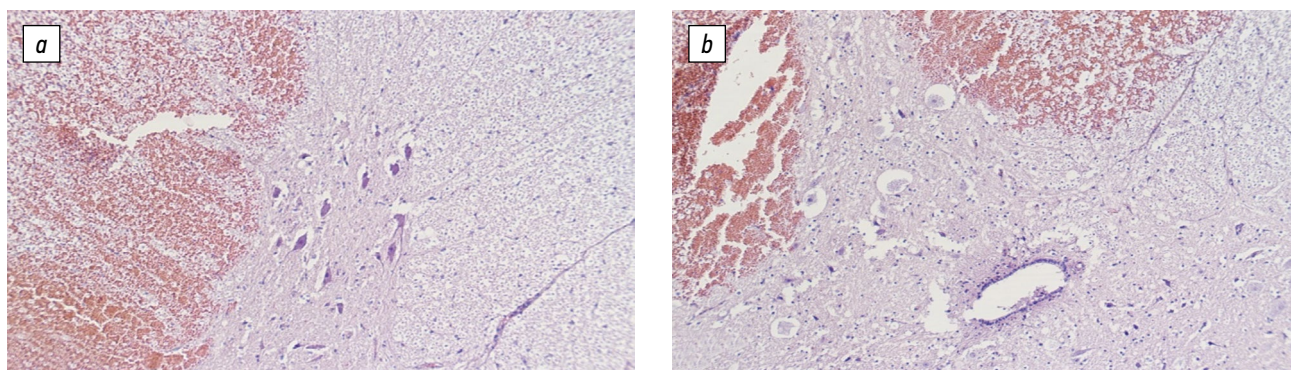


Fig. 12. Dystrophic changes in the neurons of the anterior horn of the spinal cord at injury by the dorsal approach, staining with hematoxylin and eosin: *a* and *b*, 99% of the altered neurons in the area of the anterior horn of the spinal cord (cross section, $\times 100$)

in soft cerebral membranes are represented by subarachnoid hemorrhages and focal edema.

Neuronal bodies in all samples went through dystrophic changes such as tigrolization of Nissl substance and dystrophy of the dark and light types (Fig. 11*a*). These changes became more pronounced over time from the moment of injury (Fig. 11*b* and 11*c*). When counting the number of neuronal bodies with signs of dystrophy, the following proportions were determined: in the samples taken immediately after the injury from the ventral group, the proportion of altered neurons was 38%–40%; at 3 h, the number of dystrophically altered neurons increased to 45%–48%; and at 8 h, it was 85%–90%.

In the dorsal group, this proportion was 30%–35% immediately after injury, 61%–65% at 3 h, and 95%–99% at 8 h.

In SCI specimens obtained using the dorsal approach, dystrophic neuronal changes were more pronounced in the anterior horns of the spinal cord (Fig. 12*a, b*).

After injury, all specimens showed initial signs of diffuse axonal damage such as club and bead-like thickening in axons extending 3–4 mm above and below the injury site (Fig. 13*a*). When counted semiquantitatively at 8 h, the ventral and dorsal groups showed similar signs of secondary axonopathy throughout the specimen, which was most pronounced in the anterior canaliculi below the SCI focus (Fig. 13*b, c*).

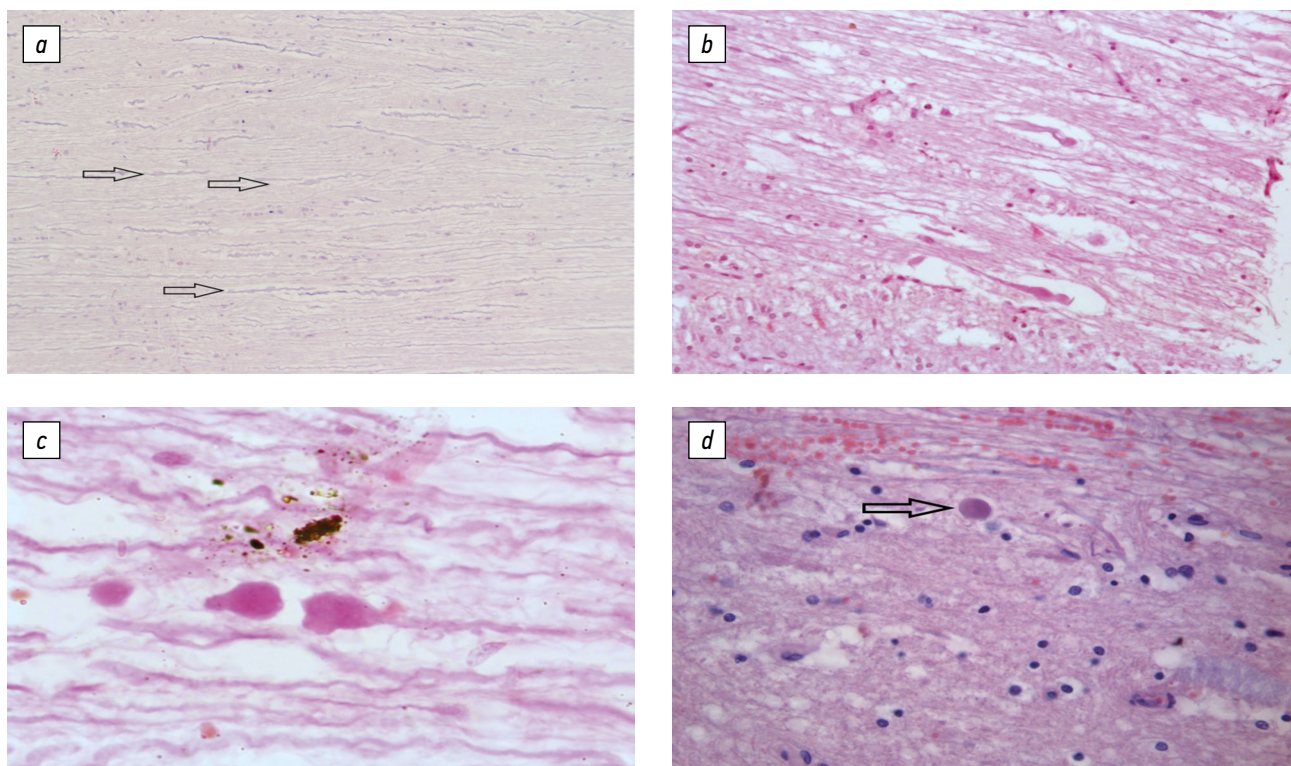


Fig. 13. Diffuse axonal damage in traumatic spinal cord injury. Longitudinal sections, hematoxylin and eosin staining: *a*, numerous thickened and deformed axons (arrows), $\times 100$; *b*, progression of the diffuse axonal damage with the formation of club-like thickening and axonal ruptures, $\times 400$; *c*, axonal rupture with the formation of eosinophilic axonal spheres, $\times 400$; *d*, amyloid cuff (arrow) at the border of gray and white matter, diffuse edema and neuropil unfolding, $\times 400$

In addition, starchy (amyloid) cells were detected in the spinal cord, which was also indicative of massive axonal damage (Fig. 13d).

DISCUSSION

This study presents the results of SCI modeling using the ventral approach in rabbits, which is more labor-intensive and complicated from the point of view of surgical technique when compared with the “classical” scheme of the dorsal approach, which is widely used in experiments on rats or rabbits. Most studies performed on rabbits have investigated ischemic damage of the spinal cord, which is associated with the peculiarities of the blood supply of the lumbar segments and the relative simplicity and convenience of the surgical technique of the prevailing models. No literature data were found regarding contusion SCI, in which the traumatizing factor would act from the ventral side, which does not allow a comparative analysis of the effectiveness of the model from the ventral approach with previously performed experiments.

Neurophysiological studies to investigate spinal cord function are found in only 17.8% of publications modeling SCI in experimental animals [4].

In this study, an experimental model of spinal cord contusion injury from a ventral approach in a laboratory animal was designed and created. This model is as close as possible to the clinical situation in which the spinal cord is traumatized from the ventral region because of the damaging impact of the fragments of a fractured vertebral body.

For comparative analysis of spinal cord abnormalities, SCI was modeled by ventral and dorsal approaches and neurophysiological examinations, including the assessment of the H-reflex and sensory and motor pathways of the spinal cord, were performed immediately and 3 and 8 h after experimental injury. After the experiment, a comparative analysis of histological changes in the spinal cord depending on the injury type was performed.

According to the results of the study of histological changes, mild hemorrhage in the lesion zone was observed in the ventral group when compared with the dorsal group. This difference may be explained by crossing vessels supplying the target segment in the ventral group. According to previous studies devoted to the comparative description of spinal cord blood supply, rabbits are characterized by a homosegmental blood supply with virtually no collaterals [11, 16, 17], which results in a smaller hematoma when the feeding arteries are crossed. In this study, the severity of other morphological changes was comparable in ventral and dorsal SCI variants, which, with mild hemorrhage, indicates a predominant contusion mechanism of ventral SCI, causing damage to spinal cord axons, and mild compression and trophic disturbances of the spinal cord due to hematoma.

The results of the neurophysiological study in rabbits with SCI showed different degrees of spinal cord damage depending on the injury type. According to SSEP data, in the dorsal group, spinal cord conduction was partially impaired immediately after injury, and after 8 h, conduction was completely interrupted because of the increasing degree of spinal cord neuron damage, which can be explained by delayed changes along with hematoma and spinal cord edema. In the ventral group, signs of complete spinal cord damage appeared immediately after injury in 90% of cases, indicating more severe damage to spinal cord axons.

At the ventral and dorsal groups 8 h after SCI, the amplitude of MEPs from the forelimb muscles and the amplitude of SSEPs from the level of lumbar thickening increased twofold, which can be explained by the reorganization of the functional activity of preserved spinal cord neurons above and below the SCI level.

The preinjury H-reflex and M-response indices obtained in the present study are comparable with data from previous studies in intact rabbits [18], indicating the accuracy of the recording techniques used and reproducibility of the experimental model. Differences in the H-reflex indices were found in rabbits depending on the injury type. For SCI from the dorsal approach, the frequency of polysynaptic responses increased in 90% of the observations, which can be explained by the disinhibition of peripheral motoneuron activity below the injury level. In contrast, the number and amplitude of polysynaptic responses were significantly reduced in the ventral group compared with those in the dorsal group, which may indicate reduced functional activity and damage to peripheral spinal cord motoneurons below the injury level and requires further study.

When analyzing the amplitudes of the H-reflex and M-response in both types of injury, a large scatter and ambiguity of the changes in the H-reflex and M-response on the left and right sides were revealed, which may be related to the small sample size of the present study and the uneven damage to the spinal cord because of its displacement during injury modeling.

In general, the results of the neurophysiological study indicated the comparability of MEP and SSEP disturbances before and after SCI with the clinical studies [19], which allows the use of these data for monitoring spinal cord function in rabbits in further experimental models of SCI aimed at developing treatment methods. In this case, ventral SCI in rabbits can be considered a more appropriate model for studying this pathology in humans.

CONCLUSIONS

In this study, an experimental model of acute contusion SCI from the ventral approach in a laboratory animal was tested. The ventral SCI model allows for a more pronounced contusion effect of damage to spinal cord structures under

experimental conditions compared with the dorsal SCI model. The developed experimental model of SCI is as close as possible to clinical practice and can be the basis for scientific research aimed at studying spinal cord changes and new surgical, pharmacological, and physical methods of treatment of chronic SCI.

ADDITIONAL INFORMATION

Funding source. None.

Conflict of interest. The authors declare no obvious or potential conflicts of interest related to the publication of this article.

Ethical review. This study was approved by the local ethics committee of the Turner National Medical Research Center for Pediatric Traumatology and Orthopedics (Protocol No. 21–4 dated November 22, 2021).

REFERENCES

1. Alizadeh A, Dyck SM, Karimi-Abdolrezaee S. Traumatic spinal cord injury: an overview of pathophysiology, models and acute injury mechanisms. *Front Neurol.* 2019;10:282. DOI: 10.3389/fneur.2019.00282
2. Tator CH. Review of treatment trials in human spinal cord injury: issues, difficulties, and recommendations. *Neurosurgery.* 2006;59(5):957–982. DOI: 10.1227/01.NEU.0000245591.16087.89
3. Verstappen K, Aquarius R, Klymov A, et al. Systematic evaluation of spinal cord injury animal models in the field of biomaterials. *Tissue Eng Part B Rev.* 2022;28(6):1169–1179. DOI: 10.1089/ten.TEB.2021.0194
4. Sharif-Alhoseini M, Khormali M, Rezaei M, et al. Animal models of spinal cord injury: a systematic review. *Spinal Cord.* 2017;55(8):714–721. DOI: 10.1038/sc.2016.187
5. Li JJ, Liu H, Zhu Y, et al. Animal models for treating spinal cord injury using biomaterials-based tissue engineering strategies. *Tissue Eng Part B Rev.* 2022;28(1):79–100. DOI: 10.1089/ten.TEB.2020.0267
6. Vissarionov SV, Rybinskikh TS, Asadulaev MS, et al. Modeling spinal cord injuries: advantages and disadvantages. *Pediatric Traumatology, Orthopaedics and Reconstructive Surgery.* 2020;8(4):485–494. (In Russ.) DOI: 10.17816/PTORS34638
7. Kjell J, Olson L. Rat models of spinal cord injury: from pathology to potential therapies. *Dis Model Mech.* 2016;9(10):1125–1137. DOI: 10.1242/dmm.025833
8. Ballermann M, Fouad K. Spontaneous locomotor recovery in spinal cord injured rats is accompanied by anatomical plasticity of reticulospinal fibers. *Eur J Neurosci.* 2006;23(8):1988–1996. DOI: 10.1111/j.1460-9568.2006.04726.x
9. Hiraizumi Y, Fujimaki E, Tachikawa T. Long-term morphology of spastic or flaccid muscles in spinal cord-transected rabbits. *Clin Orthop Relat Res.* 1990;(260):287–296.

СПИСОК ЛИТЕРАТУРЫ

1. Alizadeh A., Dyck S.M., Karimi-Abdolrezaee S. Traumatic spinal cord injury: An overview of pathophysiology, models and acute injury mechanisms // *Front. Neurol.* 2019. Vol. 10. P. 282. DOI: 10.3389/fneur.2019.00282
2. Tator C.H. Review of treatment trials in human spinal cord injury: issues, difficulties, and recommendations // *Neurosurgery.* 2006. Vol. 59. No. 5. P. 957–982. DOI: 10.1227/01.NEU.0000245591.16087.89

Authors' contribution. A.S. Shabunin and M.V. Savina, concept and design of the study, text writing, and data analysis; T.S. Rybinskikh, development of surgical technique, surgical interventions, and data analysis; A.D. Dreval and V.D. Safarov, collection and processing of data, text writing, and technical support of the experiment; P.A. Safonov, surgical interventions and data analysis; A.M. Fedjuk and D.A. Sitovskaia, collection and processing of histological materials, histomorphological study, and text writing; A.S. Baidikova and N.M. Dyachuk, surgical interventions and data collection and processing; L.S. Konkova, veterinary support and data collection and processing; O.L. Vlasova and S.V. Vissarionov, concept and design of the study and text editing of the article.

All authors made a significant contribution to the study and preparation of the article and read and approved the final version before publication.

10. Greenaway JB, Partlow GD, Gonsholt NL, et al. Anatomy of the lumbosacral spinal cord in rabbits. *J Am Anim Hosp Assoc.* 2001;37(1):27–34. DOI: 10.5326/15473317-37-1-27
11. Mazensky D, Flesarova S, Sulla I. Arterial blood supply to the spinal cord in animal models of spinal cord injury. A Review. *Anat Rec (Hoboken).* 2017;300(12):2091–2106. DOI: 10.1002/ar.23694
12. Vink R, Noble LJ, Knobloch SM, et al. Metabolic changes in rabbit spinal cord after trauma: magnetic resonance spectroscopy studies. *Ann Neurol.* 1989;25(1):26–31. DOI: 10.1002/ana.410250105
13. Sung DH, Lee KM, Chung SH, et al. Change of stretch reflex in spinal cord injured rabbit: experimental spasticity model. *Journal of the Korean Academy of Rehabilitation Medicine.* 2002;26(1):37–45.
14. Shek JW, Wen GY, Wisniewski HM. Atlas of the rabbit brain and spinal cord. Karger Basel; 1986.
15. Patent RF na izobretenie No. 2021124504 / 16.08.2021. Vissarionov SV, Rybinskikh TS, Asadulaev MS. Sposob modelirovaniya travmaticheskogo povrezhdeniya spinnoy mozga iz ventral'nogo dostupa v poyasnichnom otdel pozvonochnika. (In Russ.) [cited 2023 Nov 4]. Available from: https://i.moscow/patents/ru2768486c1_20220324
16. Mazensky D, Danko J, Petrovova E, et al. Arterial peculiarities of the thoracolumbar spinal cord in rabbit. *Anat Histol Embryol.* 2014;43(5):346–351. DOI: 10.1111/ah.12081
17. Mazensky D, Petrovova E, Danko J. The anatomical correlation between the internal venous vertebral system and the cranial venae cavae in rabbit. *Anat Res Int.* 2013;2013. DOI: 10.1155/2013/204027
18. Turan E, Ünsal C, Üner AG. H-reflex and M-wave studies in the fore- and hindlimbs of rabbit. *Turkish J Vet Anim Sci.* 2013;37(5):559–563. DOI: 10.3906/vet-1210-27
19. Gnezditskii VV, Korepina OS. Atlas po vyzvannym potentsialam mozga (prakticheskoe rukovodstvo, osnovannoe na analize konkretnykh klinicheskikh nablyudenii). Ivanovo: PresSto; 2011. (In Russ.)

3. Verstappen K., Aquarius R., Klymov A., et al. Systematic evaluation of spinal cord injury animal models in the field of biomaterials // *Tissue Eng. Part B Rev.* 2022. Vol. 28. No. 6. P. 1169–1179. DOI: 10.1089/ten.TEB.2021.0194
4. Sharif-Alhoseini M., Khormali M., Rezaei M., et al. Animal models of spinal cord injury: a systematic review // *Spinal Cord.* 2017. Vol. 55. No. 8. P. 714–721. DOI: 10.1038/sc.2016.187

5. Li J.J., Liu H., Zhu Y., et al. Animal models for treating spinal cord injury using biomaterials-based tissue engineering strategies // *Tissue Eng. Part B Rev.* 2022. Vol. 28. No. 6. P. 79–100. DOI: 10.1089/ten.TEB.2020.0267
6. Виссарионов С.В., Рыбинских Т.С., Асадулаев М.С., и др. Моделирование повреждений спинного мозга: достигнутые успехи и недостатки // *Ортопедия, травматология и восстановительная хирургия детского возраста.* 2020. Т. 8. № 4. С. 485–494. DOI: 10.17816/PTORS34638
7. Kjell J., Olson L. Rat models of spinal cord injury: from pathology to potential therapies // *Dis. Model. Mech.* 2016. Vol. 9. No. 10. P. 1125–1137. DOI: 10.1242/dmm.025833
8. Ballermann M., Fouad K. Spontaneous locomotor recovery in spinal cord injured rats is accompanied by anatomical plasticity of reticulospinal fibers // *Eur. J. Neurosci.* 2006. Vol. 23. No. 8. P. 1988–1996. DOI: 10.1111/j.1460-9568.2006.04726.x
9. Hiraizumi Y., Fujimaki E., Tachikawa T. Long-term morphology of spastic or flaccid muscles in spinal cord-transected rabbits // *Clin. Orthop. Relat. Res.* 1990. Vol. 260. P. 287–297.
10. Greenaway J.B., Partlow G.D., Gonsholt N.L., et al. Anatomy of the lumbosacral spinal cord in rabbits // *J. Am. Anim. Hosp. Assoc.* 2001. Vol. 37. No. 1. P. 27–34. DOI: 10.5326/15473317-37-1-27
11. Mazensky D., Flesarova S., Sulla I. Arterial blood supply to the spinal cord in animal models of spinal cord injury. A review // *Anat. Rec. (Hoboken).* 2017. Vol. 300. No. 12. P. 2091–2106. DOI: 10.1002/ar.23694
12. Vink R., Noble L.J., Knobloch S.M., et al. Metabolic changes in rabbit spinal cord after trauma: Magnetic resonance spectroscopy studies // *Ann. Neurol.* 1989. Vol. 25. No. 1. P. 26–31. DOI: 10.1002/ana.410250105
13. Sung D.H., Lee K.M., Chung S.H., et al. Change of Stretch reflex in spinal cord injured rabbit: experimental spasticity model duk // *Journal of the Korean Academy of Rehabilitation Medicine.* 2002. Vol. 26. No. 1. P. 37–45.
14. Shek J.W., Wen G.Y., Wisniewski H.M. Atlas of the rabbit brain and spinal cord. Karger Basel, 1986.
15. Патент РФ на изобретение № 2021124504 / 16.08.2021. Виссарионов С.В., Рыбинских Т.С., Асадулаев М.С. Способ моделирования травматического повреждения спинного мозга из вентрального доступа в поясничном отделе позвоночника [дата обращения 04.11.2023]. Доступ по ссылке: https://i.moscow/patents/ru2768486c1_20220324
16. Mazensky D., Danko J., Petrovova E., et al. Arterial peculiarities of the thoracolumbar spinal cord in rabbit // *Anat. Histol. Embryol.* 2014. Vol. 43. No. 5. P. 346–351. DOI: 10.1111/ah.12081
17. Mazensky D., Petrovova E., Danko J. The anatomical correlation between the internal venous vertebral system and the cranial venae cavae in rabbit // *Anat. Res. Int.* 2013. Vol. 2013. P. 1–4. DOI: 10.1155/2013/204027
18. Turan E., Ünsal C., Üner A.G. H-reflex and M-wave studies in the fore- and hindlimbs of rabbit // *Turkish J. Vet. Anim. Sci.* 2013. Vol. 37. No. 5. P. 559–563. DOI: 10.3906/vet-1210-27
19. Гнездицкий В.В., Корепина О.С. Атлас по вызванным потенциалам мозга (практическое руководство, основанное на анализе конкретных клинических наблюдений). Иваново: ПресСто, 2011. 532 с.

AUTHOR INFORMATION

* **Anton S. Shabunin**, MD, Research Associate;
address: 64–68 Parkovaya str., Pushkin, Saint Petersburg,
196603, Russia;
ORCID: 0000-0002-8883-0580;
eLibrary SPIN: 1260-5644;
e-mail: anton-shab@yandex.ru

Margarita V. Savina, MD, PhD, Cand. Sci. (Med.);
ORCID: 0000-0001-8225-3885;
eLibrary SPIN: 5710-4790;
e-mail: drevma@yandex.ru

Timofey S. Rybinskikh, resident;
ORCID: 0000-0002-4180-5353;
eLibrary SPIN: 7739-4321;
e-mail: timofey1999r@gmail.com

Anna D. Dreval, student;
ORCID: 0009-0007-3985-634X;
eLibrary SPIN: 4175-6620;
e-mail: anndreval@yandex.ru

Vladislav D. Safarov, student;
ORCID: 0009-0006-2948-133X;
eLibrary SPIN: 5240-1801;
e-mail: vladsafarov.vs@mail.ru

Platon A. Safonov, student;
ORCID: 0009-0006-7554-1292;
eLibrary SPIN: 6088-1297;
e-mail: safo165@gmail.com

ОБ АВТОРАХ

* **Антон Сергеевич Шабунин**, научный сотрудник;
адрес: Россия, 196603, Санкт-Петербург, Пушкин,
ул. Парковая, д. 64–68;
ORCID: 0000-0002-8883-0580;
eLibrary SPIN: 1260-5644;
e-mail: anton-shab@yandex.ru

Маргарита Владимировна Савина, канд. мед. наук;
ORCID: 0000-0001-8225-3885;
eLibrary SPIN: 5710-4790;
e-mail: drevma@yandex.ru

Тимофей Сергеевич Рыбинских, клинический ординатор;
ORCID: 0000-0002-4180-5353;
eLibrary SPIN: 7739-4321;
e-mail: timofey1999r@gmail.com

Анна Дмитриевна Древаль, студент;
ORCID: 0009-0007-3985-634X;
eLibrary SPIN: 4175-6620;
e-mail: anndreval@yandex.ru

Владислав Дмитриевич Сафаров, студент;
ORCID: 0009-0006-2948-133X;
eLibrary SPIN: 5240-1801;
e-mail: vladsafarov.vs@mail.ru

Платон Андреевич Сафонов, студент;
ORCID: 0009-0006-7554-1292;
eLibrary SPIN: 6088-1297;
e-mail: safo165@gmail.com

* Corresponding author / Автор, ответственный за переписку

AUTHOR INFORMATION

Andrey M. Fedyuk, resident;
ORCID: 0000-0002-2378-2813;
eLibrary SPIN: 3477-0908;
e-mail: Andrej.fedyuk@gmail.com

Daria A. Sitovskaia, MD, pathologist, researcher;
ORCID: 0000-0001-9721-3827;
eLibrary SPIN: 3090-4740;
e-mail: daliya_16@mail.ru

Nikita M. Dyachuk, student;
ORCID: 0009-0009-4384-9526;
e-mail: wrwtit@yandex.ru

Alexandra S. Baidikova, student;
ORCID: 0009-0008-8785-0193;
eLibrary SPIN: 7805-1341;
e-mail: baidikovaalexandra@yandex.ru

Lidia S. Konkova, MD, PhD student;
ORCID: 0009-0007-5400-3513;
eLibrary SPIN: 3527-7121;
e-mail: lidia.kireeva@yandex.ru

Olga L. Vlasova, PhD, Dr. Sc. (Phys. and Math.), Assistant Professor;
ORCID: 0000-0002-9590-703X;
eLibrary SPIN: 7823-8519;
e-mail: vlasova.ol@spbstu.ru

Sergei V. Vissarionov, MD, PhD, Dr. Sci. (Med.),
Professor, Corresponding Member of RAS;
ORCID: 0000-0003-4235-5048;
eLibrary SPIN: 7125-4930;
e-mail: vissarionovs@gmail.com

ОБ АВТОРАХ

Андрей Михайлович Федюк, ординатор;
ORCID: 0000-0002-2378-2813;
eLibrary SPIN: 3477-0908;
e-mail: Andrej.fedyuk@gmail.com

Дарья Александровна Ситовская, врач-патологоанатом;
ORCID: 0000-0001-9721-3827;
eLibrary SPIN: 3090-4740;
e-mail: daliya_16@mail.ru

Никита Михайлович Дячук, студент;
ORCID: 0009-0009-4384-9526;
e-mail: wrwtit@yandex.ru

Александра Сергеевна Байдикова, студент;
ORCID: 0009-0008-8785-0193;
eLibrary SPIN: 7805-1341;
e-mail: baidikovaalexandra@yandex.ru

Лидия Сергеевна Конькова, аспирант;
ORCID: 0009-0007-5400-3513;
eLibrary SPIN: 3527-7121;
e-mail: lidia.kireeva@yandex.ru

Ольга Леонардовна Власова, д-р физ.-мат. наук, доцент;
ORCID: 0000-0002-9590-703X;
eLibrary SPIN: 7823-8519;
e-mail: vlasova.ol@spbstu.ru

Сергей Валентинович Виссарионов, д-р мед. наук,
профессор, чл.-корр. РАН;
ORCID: 0000-0003-4235-5048;
eLibrary SPIN: 7125-4930;
e-mail: vissarionovs@gmail.com